Low-frequency Sea level changes in the Caspian Sea: long-term and seasonal trends

Jafar Azizpour (azizpour@inio.ac.ir)
Iranian National for Oceanography and Atmospheric Science
Peygham Ghaffari
Akvaplan-niva AS

Research Article

Keywords: Caspian Sea, Sea level, climate change, Spectrum analysis, decomposition method.

Posted Date: July 20th, 2022

DOI: https://doi.org/10.21203/rs.3.rs-1845231/v1

Low-frequency Sea level changes in the Caspian Sea: long-term and seasonal trends

Jafar Azizpour[1*], Peygham Ghaffari[2]
[1]Iranian National for Oceanography and Atmospheric Science, No. 3, Etemadzadeh St., Fatemi Ave., Tehran 1411813389, Iran.
ORCID iD: 0000-0003-2121-1520
[2]Akvaplan-niva AS, CIENS, Oslo, Norway.

Corresponding Author: [*]azizpour@inio.ac.ir

Abstract:

The analysis of seasonal and long-term changes of the Caspian Sea level examined from historical long time tide gauge data in order to consider the influence of climate factors on sea-level changes in this lake system. The major peak at spectra corresponds to the annual cycle and semiannual oscillations peak is located at next vigorous. Effects of diverse global and regional factors on lake level changes are investigated by signal processing methods. Results show that annual cycle of Siberian High and Volga River discharge have the considerable effects on the Caspian Sea level changes in global and regional scales, respectively. Analyzing of seasonal cycle is revealed that Volga river discharge was significant on sea level fluctuations by one-month lag in northern and central basins and two months delay for southern basin. The long-term cycle results show ascending trend of evaporation in central basin that it is the main factor to decreasing in the Caspian Sea level since 1990s.

Keywords: Caspian Sea; Sea level; climate change; Spectrum analysis; decomposition method.

1 Introduction

The Caspian Sea (CS) is largest inland water body in the earth with volume of ~78000 km^3 and a surface area of ~371000 km^2extending 1200 km from north to south, and 320 km from west to east. The Caspian Sea is surrounded by five countries: Azerbaijan, Iran, Kazakhstan, Russia, and Turkmenistan. The CS respect to physico-geographical and topography conditions divided in three sub-basins; southern, central and northern basins (Fig. 1). The Absheron sill with a maximum depth of about 170 m respectively, separates southern and central sub-basins, with a maximum water depths of about 1025 and 788 m. The northern shelf basin is a very shallow with a maximum depth of about 20 m and separated by Mangyshlak Ridge from central basin. Mean the CS level is currently approximately ~27.5 m below world ocean level (Ataei H et al., 2019; Chen et al., 2017; Ghaffari et al., 2010; Kosarev, 2005; Peeters et al., 2000; Zonn and Kostianoy, 2016).

Without a connection to the ocean, the CS level mainly controlled by rivers inflow, precipitation, evaporation and discharge to Kara-Bogaz bay. About 130 rivers flow into the CS and the main river inflow is the Volga, which discharges into the northern basin, contributing about 80% of the total river runoff (Kosarev, 2005; Roshan et al., 2012). Due to wide watershed area of the CS (~ 2500 km from north to south and about 1000 km from west to east), the CS level particularly is sensitive to climatic condition in the catchment area and inter-decadal climate fluctuations. The ratio between the CS surface area and the catchment basin (1:10) revealed that the processes proceeding in the entire basin on its natural conditions has momentous effects (Kosarev, 2005; Zonn and Kostianoy, 2016).

Over the past several years, the CS level has been characterized by significant fluctuations, including changes of several meters within the past few decades. Two sever abrupt changes of the level were observed in the previous century. A fast drop of the CS level occurred 1930s with 1.7 m has been ascribed to the Volga River discharge owing to reduction in precipitation over catchment area and dam constructions. Another fast-unexpected change happened between 1978 and 1995 that sea level rose about 2.5 m. The CS level fell about 3 m from 1929 to 1978 (Arpe et al., 2000; Beni et al., 2013; Chen et al., 2017). Consequently, changes of the CS level are important for surrounding countries, which have social, economic, maritime, and ecosystem effects.

The mean sea level changes are one of the most descriptive signs of the global climate change. The sea level changeability in each region is influenced by regional and global various factors. Regional and global climate change cause to an increase in air temperature, sea level changes, as well as to a desertification in some areas (Zonn and Kostianoy, 2016).

For analyzing global and regional signals in geophysical data sets, managing of time and frequency domain are propitious. Spectral density analysis and wavelet transform are common signal processing tools in geoscience for correlative analyzing of localized variations within a time series (Azizpour and Ghaffari, 2021). These techniques can be utilized to identify dominant regional and global processes in the CS level fluctuations. Spectral methods decompose and transport a time series from the time domain into the frequency domain, where it is possible to determine both dominant modes of variability and how those modes vary in time (Grinsted et al., 2004). It is possible to capture localized energies using wavelet technics, which indicate the exact signal-occurrence time by translating signals into the time domain.

In global and regional scales, most of the teleconnection indices (usually defined as anomalies of a climatic variable) can serve as prognostic tools based on their ability to explain the climatic variability of a region, particularly when they influence on sea hydrodynamics (Criado-Aldeanueva and Soto-Navarro, 2013b; Lopez-Bustins et al., 2008). In this paper, effects of local and global signals on the Caspian Sea level changes are investigated using wavelet analysis methods. In addition, Caspian Sea level changes in different cycles and effects of climate changes on the Caspian Sea are considered in three distinct basins i.e. northern, central, and southern basins.

2 Material and methods

The CS level changes are investigated based on historical tide gauge data. In the CS as an enclosed basin, sea level variations are controlled by river discharge, total precipitations, and evaporation (Chen et al., 2017). The CS extends from 36° to 47° and 47° to 54° in the North and East directions, respectively, located within an endorheic basin between Europe and Asia, the CS is surrounded by five countries: Russia, Kazakhstan, Turkmenistan, Iran, and Azerbaijan (Figure 1) and it divides in three distinct basins (Ghaffari et al., 2010). Differences between the three sub-basins are dramatic. Rate of evaporation and precipitation in distinct sub-basins of the CS are completely different and so we study basins separately.

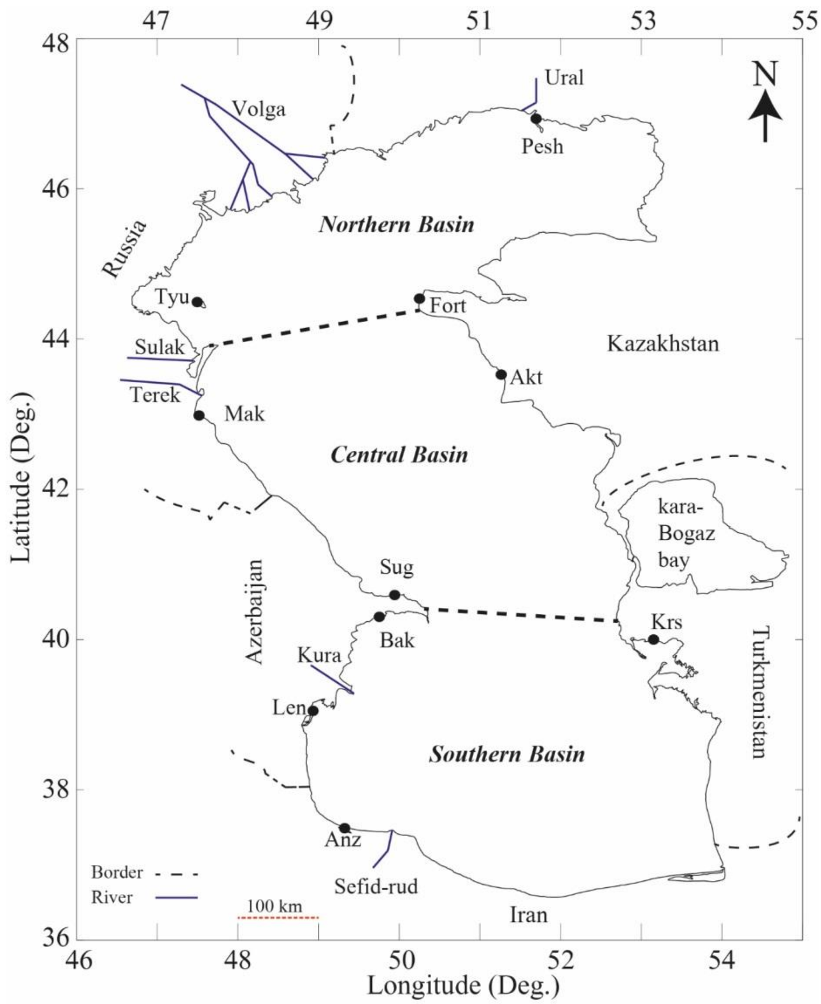

Figure 1. The Caspian Sea with three distinct basins and main rivers

2.1 Data set

2.1.1 **Regional scale factors**

Historical monthly records of sea level fluctuations from tide gauge measurements, air temperature, water temperature and *in-situ* river discharge at several different stations in the three distinct basins (Fig. 1) of the CS are used. The period of monthly data for sources and stations are different and extended from early 1900 to end 2017 (see Table 1). Evaporation and total precipitation monthly mean data are downloaded from ECMWF ERA5 data set (https://cds.climate.copernicus.eu) from 1950 to end 2017. Recently ECMWF extended meteorological data from 1950 to end 1978. For generating coherency, graphs between CS level and regional factors data are used from 1950 to end 2017.

Table 1. Stations of different basins in the Caspian Sea, the dates show available data periods.

	Basin	Regional Parameters (Period)			
		River discharge	**Water level**	**Air temperature**	**Water temperature**
station	**North**	Volga (1938-2017)	Fort Shevchenko (1921-2017)	Peshnoy (1940-2017)	Tyuleniy Island (1961-2017)
	Central	Terek (1965-2017)	Makhachkala (1900-2017)	Makhachkala (1900-2017)	Aktau (1977-2017)
	South	Kura (1946-2009)	Krasnovodsk (1915-2017)	Anzali (1952-2017)	Baku (1961-2012)

2.1.2 Global scale factors

For investigating about effects of global factors on the CS level fluctuations, different monthly mean data sources consists of Arctic oscillation (AO) index, North Atlantic Oscillation (NAO), Southern Oscillation Index (SOI), Siberian High (SH), and Western Mediterranean Oscillation (WMO) index are used.

The AO index is a climate pattern considered by winds circulating counterclockwise around the Arctic at around 55°N latitude. In positive phase of the AO, strong winds act around the North Pole that confine colder air across Polar Regions. This belt of winds becomes weaker and more distorted in the negative phase of the AO, which allows an easier southward penetration of colder, arctic air masses and increased storminess into the mid-latitudes (Thompson and Wallace, 1998).

The NAO is a standardized index based on the surface sea-level pressure difference between the Azores High and the Subpolar Low. The positive phase of the NAO reflects below-normal heights and pressure across the high latitudes of the North Atlantic and above-normal heights and pressure over the central North Atlantic. The negative phase reflects an opposite pattern of height and pressure anomalies around the North Atlantic region (Hurrell et al., 2003; Rousi et al., 2020).

The SOI index is based on the observed sea level pressure differences between Tahiti and Darwin, Australia. The SOI is one measure of the large-scale fluctuations in air pressure occurring between the western and eastern tropical Pacific during El Niño and La Niña episodes (https://www.ncdc.noaa.gov/teleconnections/enso/indicators/soi/).

The SH is a semi-permanent anticyclone centered over Eurasia and it is associated with some of the coldest, densest air masses in the Northern Hemisphere. The SH is of greater intensity than the pressure systems of the North Atlantic and North Pacific regions (Sahsamanoglou et al., 1991). Radiative cooling over snow-covered Eurasia maintains the large-scale descending motion of SH and makes it stronger in wintertime (Ding and Krishnamurti, 1987).

The WMO is defined within the synoptic framework of the western Mediterranean basin and its vicinities. The suggested areas are the Po plain, in the north of the Italian peninsula, an area with a relatively high barometric variability due to the different influence of the central European anticyclone and the Liguria low; and the Gulf of Cádiz, in the southwest of the Iberian peninsula, often subject to the influence of the Azores anticyclone and, episodically, to the cut off of circumpolar lows or to its own cyclogenesis (Criado-Aldeanueva and Soto-Navarro, 2013a; Martin-Vide and Lopez-Bustins, 2006; Palutikof, 2003).

2.2 Data processing

Atmospheric parameters synthetic dataset passed through a twofold quality control processes by 1) visual inspection and removing spikes and 2) flagging out and doublechecking data point that falls beyond 2-fold standard deviation. Small gaps in the records (<3 months) are replaced by linear interpolation of the adjacent values. Longer gaps are closed by an iterative process based on discrete cosine transform method (Garcia, 2010; Wang et al., 2012).

To study the periodical component of the data sets, spectral density analysis is performed based on the fast Fourier transform. Stochastic spectral analyses commonly are used to estimate the distribution of a parameter variance, i.e. energy, over the frequency domain. Depending on the nature of the oscillations, the spectrum can have a continuous character of the energy distribution or the form of sharp delta-like peaks (Azizpour and Ghaffari, 2021).

The spectrum of energy distribution often contains essential information about the nature of physical processes and events in a time series. However, gives no information on the temporal variation of the events. To capture and investigate temporal variations of low-frequency the CS level oscillations, we applied the wavelet signal processing method.

A wavelet $\psi(t)$ is a function, oscillates with zero-mean around *t-axis*, which contains both frequency and time and loses strength as it moves away from the mean. A wavelet can be described based on its localization in time (Δt) and frequency (Δf, or the bandwidth). One common wavelet is the mother, defined by:

$$\psi_{a,b}(t) = |a|^{-\frac{1}{2}}\psi\left(\frac{t-b}{a}\right), a, b \in R, a \neq 0. \quad (1)$$

The mother wavelet is expanded to form a basis for Hilbert space. In relation (1), ψ is mother wavelet, b is a position parameter, and a is a scaling parameter. $|a|^{-\frac{1}{2}}$ is a normalizing constant. Consequently, continuous wavelet transform is given by

$$w(a,b) = |a|^{-\frac{1}{2}}\int_{-\infty}^{\infty} f(t)\,\psi\left(\frac{t-b}{a}\right)dt, a, b \in R, a \neq 0, \quad (2)$$

where, $w\ (a, b)$ are called wavelet coefficients (Hariharan, 2019). It decomposes the time series into time-frequency space and reveals all dominant modes of the variability and the way these modes change in time.

In this study, we utilized the wavelet coherence method (Grinsted et al., 2004; Jevrejeva et al., 2005; Torrence and Compo, 1998) to investigate possible direct links between the

CS level and global such as Arctic oscillation, North Atlantic Oscillation, Southern Oscillation, Siberian High and Western Mediterranean Oscillation indexes and regional signals such as Volga River discharge, precipitation, evaporation and air temperature. Among the diverse wavelet functions, Morlet is one of the popular wavelets in geoscience studies that define as:

$$\psi_0(\eta) = \pi^{-1/4} e^{i\omega_0\eta} e^{-1/2\eta^2}, \quad (3)$$

where ω_0 and η are the dimensionless frequency and time, respectively. We utilized Morlet continuous wavelet transform for signal decomposing of diverse time series in this study.

For the analysis of the climate cycle time series, it is useful to employ mathematical equations. A simple climate equation is

$$y(i) = y_{trend}(i) + x(i) \times y_{noise}(i) \quad (4)$$

Equation (4) decomposes climate cycle data into a trend and noise components, which the noise component has mean zero (Mudelsee, 2019). Here we employed equation (4) to decompose trend slope from long-term time series by linear least square regression method.

3 Results

3.1 Spectral analysis

Historical tide gauge data of the CS level revealed that this basin's level changes were about 3m from 1900 to 2017. From 1900s to 1970s sea level are decreased three times with 6.53, 19.86 and 5.45 cm/yr, respectively. Rapid decrease is occurred in 1930s. From late 1978 to late 1996, a sharp increase is happened with 16.08 cm/yrgradient and again after that time the CS level is fallen dramatically by 14.02 cm/yr slope (Fig. 2A). The CS level is affected by regional and global factors in different time scales. Figure 2B illustrates the spectra of sea level for the CS. The major peak at spectra corresponds to the annual cycle and semiannual (6 months) oscillations is located at next vigorous. For long-term oscillations, some peaks are visible at 4 to 7, 14 and around 30 years periods, respectively. The amplitudes of higher seasonal harmonics (except 4 months period) are small and it is difficult to detect them in the background noise at the spectra. Ranges of tidal constituents in the CS are less than 10 cm (Medvedev, 2019) and their energy in spectra are not detectible from background noise.

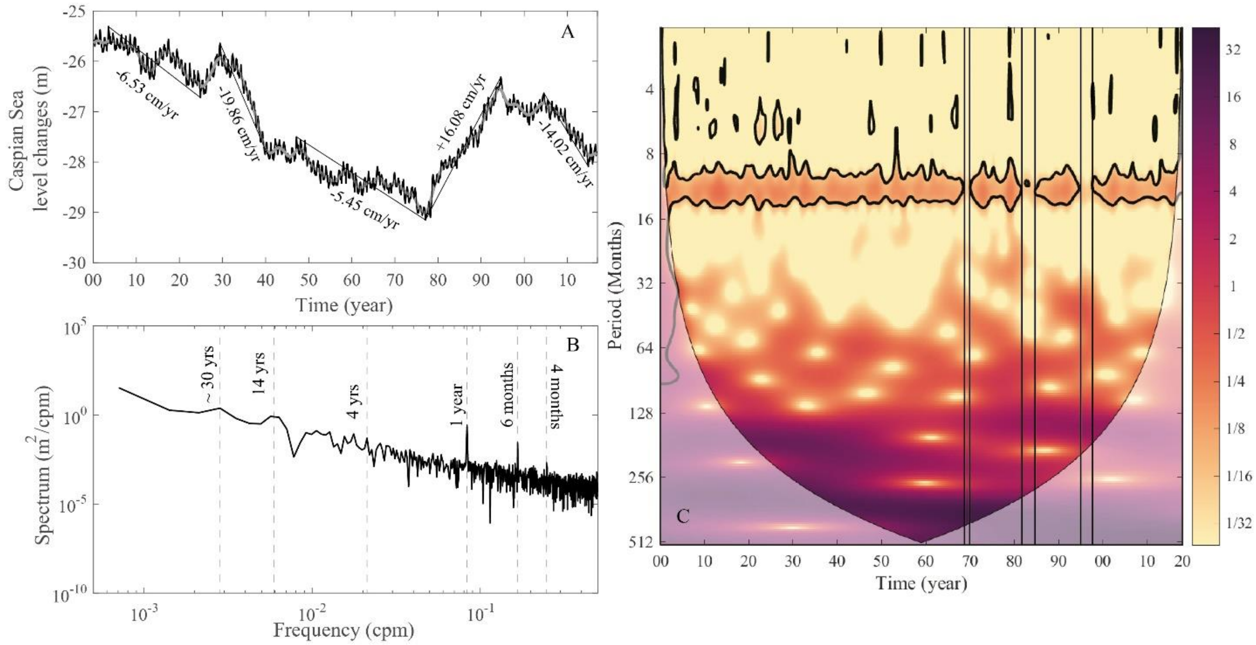

Figure 2. A) Monthly Caspian Sea level changes recorded by tide gauges and related trends (peak to peak) from 1900 to 2017 behind yearly low-passed data (gray line), B) the Caspian Sea level spectra generated by sea level data, and C) Morlet wavelet power spectrum of the sea level data.

Figure 2C shows wavelet power spectrum for monthly CS level changes from 1900 to 2017, where the strong non-stationary behavior of the spectra is obvious. The results confirm the pick signals of power spectrum analysis by revealing events on the annual, semi-annual scales. High energetic signals are appeared in long periods (more than 128 months) that Fig. 2B reveals, too. In some years, annual signal are absent in wavelet spectrum e.g. 1969-1970, 1981-1985 and 1996-1998 (vertical line in Fig. 2C). For two first periods, semi-annual signal of evaporation was dominant (Fig. 4A) and for the last one period, the NAO annual period effects on CS level is increased (Fig. 3B).

3.2 Wavelet analysis

Wavelet coherency between Synchronous monthly the CS level and global teleconnection indices from 1950 to end 2017 are shown in figure 3. All teleconnection indices, to some waiver, have direct annual, semiannual, and seasonal effects on the CS level fluctuations. The strong annual AO index effects on the CS level are happened from 1960 to 1965, around 1980 and 2003 and from 1989 to 1995. The phase of the former was in-phase and the latter was anti-phase. In the anti-phase lag, water level is increased and vice versa. In semi-annual and seasonal frequency bands, every each decade, there were at least one peak and strongest is observed around year 1970. For more than one year period, an influential is occurred from 1964 to 1971. In this period, the CS level is dropped (in-phase). Figure 3B illustrates wavelet coherency between the CS level and NAO index. Effects of NAO index on the CS level was considerable for annual and less than four years period from late 1980s to late 2015. Another high coherency is happened in 6-10 years period, from 1950 to 1975. Pattern of the SO index coherency is rather similar to NAO index (Fig. 3C), however effects of low-frequency band in the SO index was stronger. Strong effects occurred in the annual frequency band, particularly, between the CS level and the SH (Fig. 3D). In this frequency band, phase of coherency, primarily, was negative (anti-phase). Effects of the SH in seasonal and semi-annual frequency band was feeble and ignorable. In addition, for 3-7 years period, effects of the SH from late 1960s to early 2000 was remarkable.

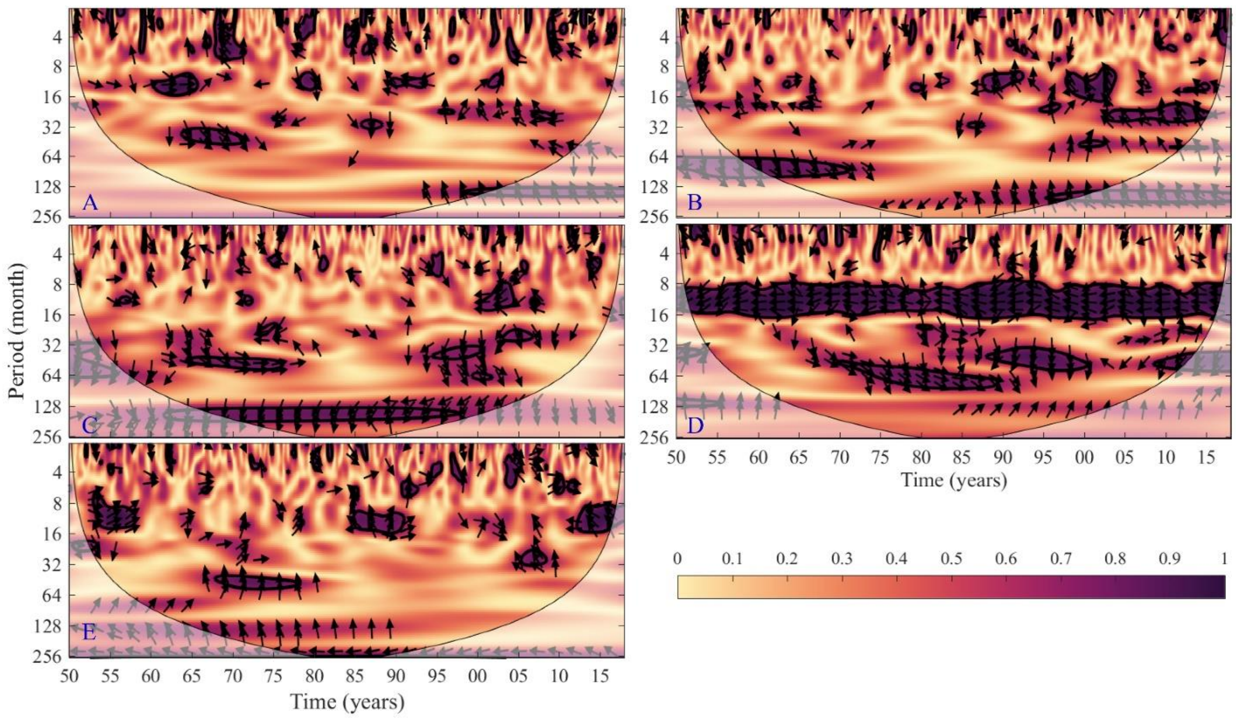

Figure 3. Wavelet coherence and the phase difference between the Caspian Sea monthly mean level data and A) Arctic oscillation, B) North Atlantic Oscillation, C) Southern Oscillation, D) Siberian High and E) Western Mediterranean Oscillation indexes.

Wavelet coherency and phase difference between CS level and the WMO index are shown in Fig. 3E. In annual period band, some strong coherencies with different phase are happened. The first, second and third coherencies are occurred in 1950s (positive phase), from 1985 to 1992 and from 2012 to 2017, respectively. Strong coherency is occurred in four years period band from 1967 to 1978. The effects of WMO index on CS level changes in semi-annual and seasonal period were considerable from 1990s to 2010.
Effects of regional factors (evaporation, total precipitation Volga River discharge and air temperature) on the CS level are investigated from 1950 to 2017 by monthly synchronous time series based on wavelet coherence analysis (Fig. 4). Annual cycle band has the dominant coherency between CS level and all regional factors that the CS level leading evaporation by 90°. Rather decussate, five years period, semiannual cycle between CS level and evaporation has also strong coherency (Fig. 4A). Another strong coherency is

occurred from 1990s to late 2000s for 2 to ~ 8 year's periods by in-phase mode. It seems that the contribution of evaporation on the CS level changes is increased since 1990s.

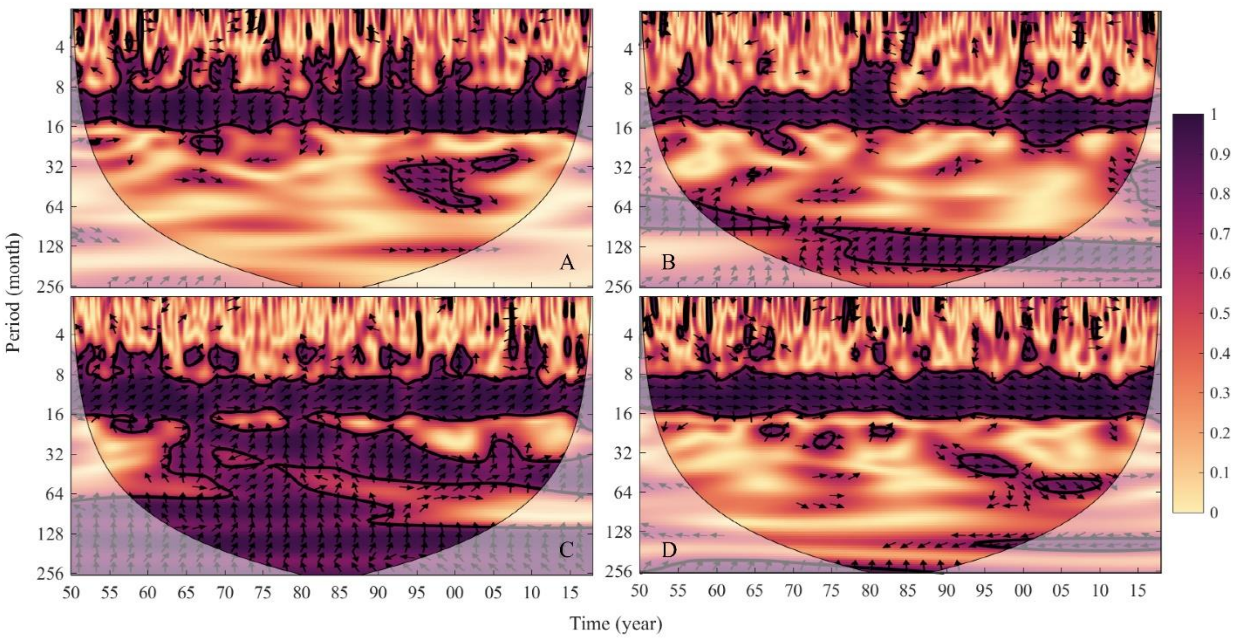

Figure 4. Wavelet coherence and the phase difference between the Caspian Sea monthly mean level and A) evaporation, B) precipitation, C) Volga river discharge, and D) air temperature.

Figure 4B shows wavelet coherence and the phase difference between the CS level and total precipitation. Effects of total precipitation in annual cycle were similar to evaporation and a strong coherency is happened in semiannual cycle from 1978 to 1983. Portion of seasonal component was not significant and only strong coherency is observed around 1985. For five to about 10 year's period cycle (except 1970s), an intense coherency is situated at all times. Strong coherency is occurred between the CS level and Volga River discharge in several frequency bands. Generally seasonal period band was not important, while semiannual period has rather strongly coherency, especially 1950s, and around year's 1970, 1981, 1992, 2002 and 2011 (Fig. 4C). Pattern of wavelet coherency between CS and air temperature (Fig. 4D) are very similar to evaporation for annual and longer period bands. Strongest coherency is occurred in annual band in all times. Another strong coherencies are took place in three and four year's periods from

1992 to 1998 and 2001 to 2010, respectively. Phase of annual and two recent coherencies were in positive phase.

3.3 Mean seasonal cycle

The mean seasonal cycle is computed for each monthly evaporation, total precipitation, sea level tide gauge record for three distinct basins and Volga River discharge by averaging the values for each calendar month. Figure 5 shows the mean seasonal cycle over the complete period 1950 to end 2017. Rate of evaporation in distinct basins of the CS is individually different (Fig. 5A, D and G). The pattern of the evaporation rate for central and southern basins are rather similar, although rate of southern basin is larger than central basin .Maximum quantity of evaporation is took place in the northern basin in the July, while for the central and southern basins are occurred in the September. Similar to evaporation, for total precipitation graphs are illustrated in Fig. 5B, E, and H. The maximum amount of total precipitation are took place in the winter and fall seasons and from north to south, amount of total precipitation has an increasing trend. The mean seasonal pattern for total precipitation exhibits a clear latitudinal dependence with the amplitude increasing southward.

The mean seasonal cycle for sea level fluctuations has a different manner comparing with evaporation and total precipitations i.e. maximum quantities of sea level are recorded when amount of evaporation was maximum while total precipitation amount was minimum (Fig. 5C, F and I). Rather by one-month lag, pattern of sea level and Volga River are the same. Maximum amount of river discharge is recorded in May (Fig. 5J) and for sea level in northern and central basins it is recorded in June while for southern basin it is took place in July. Consequently, seasonal variability of sea level in the Caspian Sea is strongly determined by Volga River discharge.

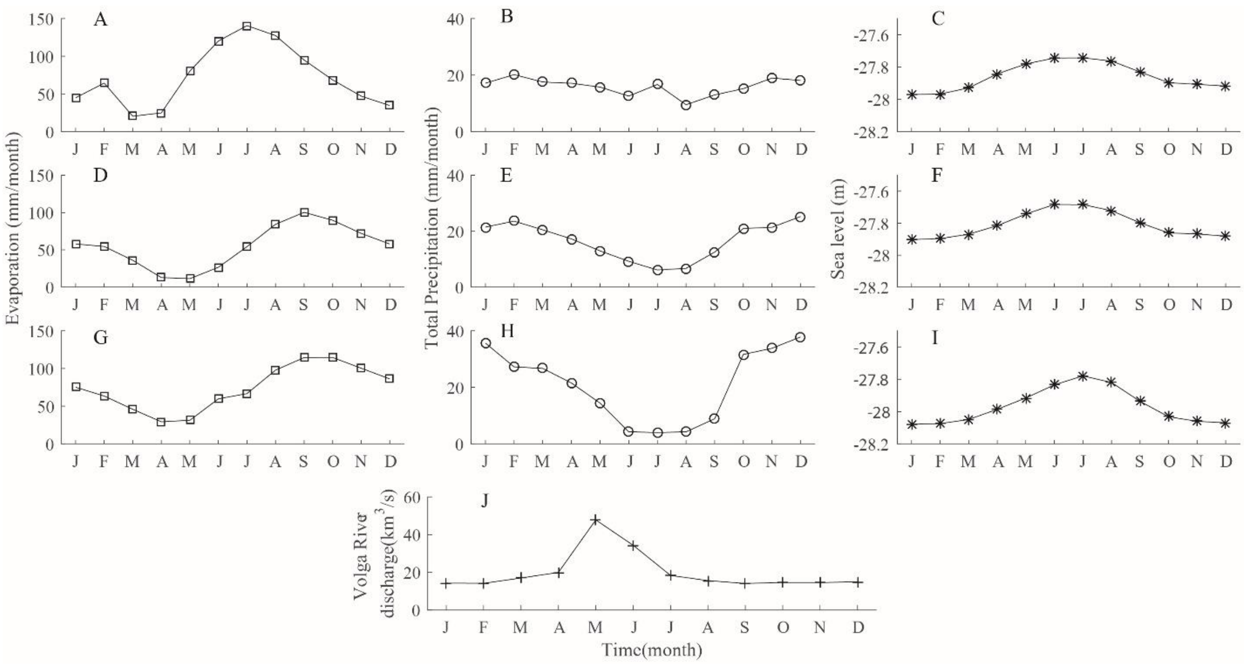

Figure 5. Mean seasonal cycle (1950-2017) for evaporation ($mm/month$) in A) north basin, D) Central Basin, G) southern basin, total precipitation ($mm/month$) in B) north basin, E) Central Basin, H) southern basin, sea level changes (m) in C) north basin, F) Central Basin, I) southern basin and J) Volga River discharge (km^3/s).

3.4 Climate cycle

For analyzing climate change effects on different parameters in three distinct basins of the CS, long-term time series of evaporation, total precipitation, air temperature, water temperature and also river discharges are presented in figure 6. The slope of evaporation trend for central basin was larger than two other basins. In fact, since 1990s the evaporation rate is increased impressive in central basin. Generally, slope of evaporation trend's for three basins were ascending since 1950 to end 2017. Commonly the amount of total precipitation trend slopes were ascending but the least total precipitation is took place in central basin, which in this basin maximum slope is observed for evaporation. Increasing in total precipitation was considerable in northern basin (m = 0.00013) that it was at least 1.5 times greater than other basins. Around year 1980, quantities of evaporation in whole the CS is decreased, while the amount of total precipitation is increased and these were may be some of reasons to increase in CS level in that time.

Third row of figure 6 shows air temperature time series in Peshnoy (northern basin), Makhachkala (central basin) and Anzali port (southern basin) by different periods. The slopes of linear trend were ascending similar to evaporation and total precipitation. Effects of clime change on air temperature in the northern basin was remarkable.

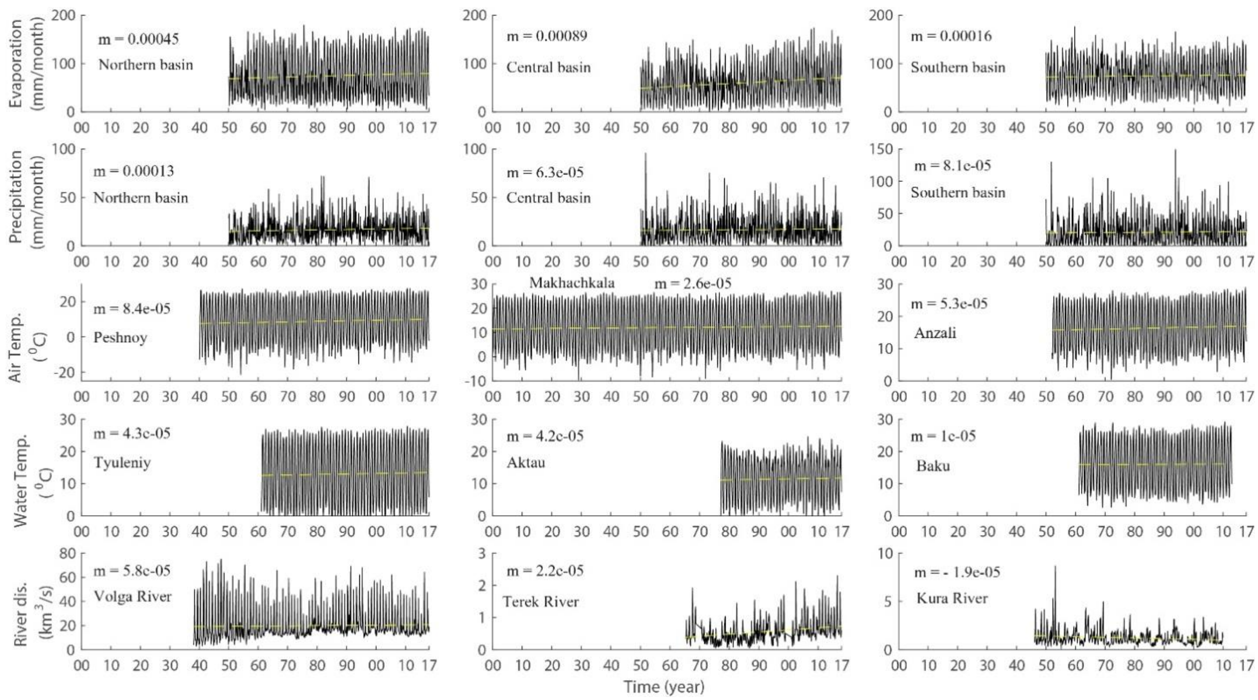

Figure 6. Monthly records for different parameters in the three distinct basins of the CS, first column for northern basin, second column for central basin and third column is related to southern basin. The dashed red line depicts the linear trend estimated for each record by ordinary least squares. The m amounts indicate to each trend slope.

The same pattern is observed for water temperature in entire CS. Water temperature in the selected stations is increased in three basins. Similar to air temperature, water temperature trend's slope in the northern basin (Tyuleniy station) was greater than other basins (although measurements time were not synchronizes). Due to the northern basin is shallow and average depth of it is about 5m, it strongly affected by environmental factors. Except Kura River, trend of Volga and Terek rivers discharge were ascending. The Volga River is the main discharge source in the CS and it has greatest slope in compare with other rivers (m = 5.8 e -5). Though over time, the maximum quantities of Volga River discharge is decreased, but simultaneously minimum amounts of discharge is increased and over all from 1938 to 2017 it has increasing slope.

4 Conclusion

The monthly mean long-term Caspian Sea level changes are discussed by signal analysis processing method. The cross wavelet analysis is revealed that maximum coherency between the Caspian Sea level and regional and global factors is occurred in annual period. Moreover maximum coherency between the Caspian Sea and regional and global factors were Volga River discharge and Siberian High, respectively.

The mean seasonal cycle of sea level variability in the Caspian Sea is characterised by a clear minimum in winter and a maximum, which occurs in late spring for the northern and central basins and in early summer for the southern basin. The Volga River discharge has key effect on Caspian Sea level in seasonal cycle by 1-2 month delay.

Effects of global warming (climate change) are observed in evaporation, total precipitation, air temperature; water temperature and surrounding Caspian Rivers by ascending trend in three distinct basins. Although slope of all mentioned parameters (except Kura River discharge) in three basins of the Caspian Sea were ascending, but trend of Caspian Sea level were descending. One of main reasons may be increasing in evaporation rate in the whole Caspian basin, especially central basin since mid-1990s, and it essentially depends on wind speed. Serykh and Kostianoy (2020) is illustrated that since 1995, the negative anomalies of zonal wind cause to the evaporation growth and the sea level drop. Signature of the climate change has been manifested in the CS since 1995 attributed to the higher frequency of crossing Central Asia dry winds over the CS which is accompanied by higher sea surface evaporation (Serykh and Kostianoy, 2020).

Acknowledgement:

This work supported by Iranian National Institute for Oceanography and Atmospheric Science (project code: INIOAS-1400-012-01-44-04). We gratefully acknowledge them for supporting this project.

References

Arpe K, Bengtsson L, Golitsyn G, Mokhov I, Semenov V, Sporyshev P (2000) Connection between Caspian Sea level variability and ENSO. Geophysical Research Letters 27:2693-2696.

Ataei H S, Jabari Kh A, Khakpour AM, Neshaei SA, Yosefi Kebria D (2019) Long-term Caspian Sea level variations based on the ERA-interim model and rivers discharge. International Journal of River Basin Management 17:507-516.

Azizpour J, Ghaffari P (2021) Global and regional signals in the water level variation in Hypersaline Basin of the Lake Urmia. Springer.

Beni AN, Lahijani H, Harami RM, Arpe K, Leroy S, Marriner N, Berberian M, Andrieu-Ponel V, Djamali M, Mahboubi A (2013) Caspian sea level changes during the last millennium: historical and geological evidences from the south Caspian Sea.

Chen J, Pekker T, Wilson CR, Tapley B, Kostianoy A, Cretaux JF, Safarov E (2017) Long-term Caspian Sea level change. Geophysical Research Letters 44:6993-7001.

Criado-Aldeanueva F, Soto-Navarro F (2013a) The Mediterranean Oscillation Teleconnection Index: Station-Based versus Principal Component Paradigms, Adv. Meteorol., 2013, 1–10.

Criado-Aldeanueva F, Soto-Navarro FJ (2013b) The Mediterranean Oscillation teleconnection index: station-based versus principal component paradigms. Advances in Meteorology 2013.

Ding Y, Krishnamurti TN (1987) Heat budget of the Siberian high and the winter monsoon. Monthly weather review 115:2428-2449.

Garcia D (2010) Robust smoothing of gridded data in one and higher dimensions with missing values. Computational statistics & data analysis 54:1167-1178.

Ghaffari P, Lahijani H, Azizpour J (2010) Snapshot observation of the physical structure and stratification in deep-water of the South Caspian Sea (western part). Ocean Science 6:877-885.

Grinsted A, Moore JC, Jevrejeva S (2004) Application of the cross wavelet transform and wavelet coherence to geophysical time series.

Hariharan G (2019) Wavelet Analysis—An Overview. Wavelet Solutions for Reaction–Diffusion Problems in Science and Engineering. Springer, pp. 15-31.

Hurrell JW, Kushnir Y, Ottersen G, Visbeck M (2003) An overview of the North Atlantic oscillation. Geophysical Monograph-American Geophysical Union 134:1-36.

Jevrejeva S, Moore J, Woodworth P, Grinsted A (2005) Influence of large-scale atmospheric circulation on European sea level: results based on the wavelet transform method. Tellus a: Dynamic Meteorology and Oceanography 57:183-193.

Kosarev AN (2005) Physico-geographical conditions of the Caspian Sea. The Caspian Sea Environment. Springer, pp. 5-31.

Lopez-Bustins J-A, Martin-Vide J, Sanchez-Lorenzo A (2008) Iberia winter rainfall trends based upon changes in teleconnection and circulation patterns. Global and Planetary Change 63:171-176.

Martin-Vide J, Lopez-Bustins JA (2006) The western Mediterranean oscillation and rainfall in the Iberian Peninsula. International Journal of Climatology: A Journal of the Royal Meteorological Society 26:1455-1475.

Mudelsee M (2019) Trend analysis of climate time series: A review of methods. Earth-Science Reviews 190:310-322.

Palutikof J (2003) Analysis of Mediterranean climate data: measured and modelled. Mediterranean Climate. Springer, pp. 125-132.

Peeters F, Kipfer R, Achermann D, Hofer M, Aeschbach-Hertig W, Beyerle U, Imboden DM, Rozanski K, Fröhlich K (2000) Analysis of deep-water exchange in the Caspian Sea based on environmental tracers. Deep Sea Research Part I: Oceanographic Research Papers 47:621-654.

Roshan G, Moghbel M, Grab S (2012) Modeling Caspian Sea water level oscillations under different scenarios of increasing atmospheric carbon dioxide concentrations. Iranian journal of environmental health science & engineering 9:24.

Rousi E, Rust HW, Ulbrich U, Anagnostopoulou C (2020) Implications of Winter NAO Flavors on Present and Future European Climate. Climate 8:13.
Sahsamanoglou H, Makrogiannis T, Kallimopoulos P (1991) Some aspects of the basic characteristics of the Siberian anticyclone. International Journal of Climatology 11:827-839.
Serykh, I. V., & Kostianoy, A. G. (2020). The links of climate change in the Caspian Sea to the Atlantic and Pacific Oceans. Russian Meteorology and Hydrology, 45(6), 430-437.
Thompson DW, Wallace JM (1998) The Arctic Oscillation signature in the wintertime geopotential height and temperature fields. Geophysical Research Letters 25:1297-1300.
Torrence C, Compo GP (1998) A practical guide to wavelet analysis. Bulletin of the American Meteorological society 79:61-78.
Wang G, Garcia D, Liu Y, De Jeu R, Dolman AJ (2012) A three-dimensional gap filling method for large geophysical datasets: Application to global satellite soil moisture observations. Environmental Modelling & Software 30:139-142.
Zonn I, Kostianoy A (2016) The Caspian Sea basin. Chow's handbook of applied hydrology, 2nd rev edn. McGraw-Hill Education, Columbus, OH.

Statements and Declarations

The authors declare that they have no known competing financial interests or personal relationships that could have appeared to influence the work reported in this paper.

Funding

The authors declare that no funds, grants, or other supports were received during the preparation of this manuscript.

Competing Interests

The authors have no relevant financial or non-financial interests to disclose.

Authors Contributions

- *Jafar Azizpour: main idea, writing, data analysis, plot figures*
- *Peygham Ghaffari: data analysis, writing, editing text*

Data Availability

Data are used in this paper are common data in atmosphere and ocean science and are available in internet and data are available upon request.